Xα-SW calculation, but the spherical averaging of the potential in these calculations prevents them from displaying their full effect.

Conclusions

Although the small basis set and limited CI precludes accurate values for the IP's, we have shown that some account of the differential correlation energy may be necessary before the correct order of the ionic states is obtained. The inversion of the order of the ionic states compared to that predicted by KT occurs for two reasons. First, the IP of the mainly metal d electrons is predicted to be too large because KT fails to account for the large shielding provided by these compact d orbitals.[37] Thus, there is a huge reduction in the predicted IP of these electrons at the ΔSCF level. Second, there is a substantial differential correlation energy between the two types of ionic states. In the molecule the highly delocalized metal-Cbd electrons are not as well described by the simple MO formalism as are the localized metal electrons. The loss of this near-degenerate type of correlation when a hole is created in the delocalized metal-Cbd orbitals gives rise to an increase in the predicted IP. The differential correlation effects are overestimated by our procedure because the CI was designed primarily to correlate the electrons in the metal-Cbd bonds. The ground state of $(\eta^4\text{-}C_4H_4)Fe(CO)_3$ at the CI level provides insight into the nature of the cyclobutadiene-metal interaction and correctly accounts for the aromatic character of the metal-bound cyclobutadiene, the nucleophilic character of the Cbd ring, and the tilt of the ring system.

Acknowledgment. This work was supported by the National Science Foundation (Grant No. CHE 79-20993) and the Robert A. Welch Foundation (Grant No. A-648).

Registry No. 1, 12078-17-0.

(37) Calabro, D. C.; Lichtenberger, D. L. *Inorg. Chem.* **1980**, *19*, 1732.

Contribution from the Christopher Ingold Laboratories, University College London, London WC1H 0AJ, U.K.

On the Nature of the Sulfur Chromophores in Ultramarine Blue, Green, Violet, and Pink and of the Selenium Chromophore in Ultramarine Selenium: Characterization of Radical Anions by Electronic and Resonance Raman Spectroscopy and the Determination of Their Excited-State Geometries

ROBIN J. H. CLARK,* TREVOR J. DINES, and MOHAMEDALLY KURMOO

Received January 4, 1983

By a combination of electronic and resonance Raman spectroscopy, it is shown that the key chromophores in ultramarine green are S_3^- and S_2^- and that various forms of ultramarine violet as well as ultramarine pink contain S_3^- and S_2^- together with a third chromophore, not certainly characterized. This last species, for which λ_{max} = 520 nm, predominates in all the violet and pink forms, especially in the latter. Ultramarine selenium, which is brick red (λ_{max} = 490 nm), readily yields a single long progression (to 13 members) under resonance Raman conditions; the progression is identified as arising from the Se_2^- ion, for which the following spectroscopic constants were established: $\omega_e = 329.6 \pm 0.3$ cm^{-1}, $\omega_e x_e = 0.70 \pm 0.03$ cm^{-1}. Excitation profiles of all resonance-enhanced bands have been measured and fitted to a Franck-Condon model for the intensity of the scattering. From the best fit between calculated and observed excitation profiles, values for the change in the equilibrium S-S and Se-Se bond lengths on excitation to the resonant excited state in each case were calculated to be 0.30 ± 0.01 and 0.32 ± 0.02 Å, respectively.

Introduction

The nature of the species responsible for the blue color formed ($\lambda_{max} \simeq 600$ nm, $\epsilon_{max} \simeq 10^4$ M^{-1} cm^{-1}) when alkali metal polysulfides are dissolved in donor solvents such as dimethylformamide or hexamethylphosphoramide has recently been established[1] to be the radical anion S_3^-. No salts of this anion have ever been prepared, owing to the very rapid dimerization of the ion when usually appropriate counterions are added to its solutions. The same species has been identified as being responsible for the deep blue color of sulfur dissolved in a LiCl-KCl eutectic, in CsCl-$AlCl_3$ or KNCS melts, in the aluminosilicate mineral lapis lazuli, and in its synthetic equivalent ultramarine blue.[2-5] The last is an important chemical in the pigment industry, owing to the richness and durability of its royal blue color. Small quantities of the S_2^- ion (λ_{max} = 380-400 nm) have also been shown to be present in ultramarine blue.[1] Ultramarine green has been shown to contain the same two chromophores as the blue but in more nearly comparable proportions.[1]

By modification to the preparative procedures it is possible to make various shades of ultramarine violet, as well as ultramarine pink (or red). The nature of the species present in these forms of ultramarine is not fully understood, nor is it known whether the proportions of the chromophores change continuously or stepwise from one shade of ultramarine to another.

It has, moreover, been known since the 1920s that selenium can replace sulfur in ultramarine with only minor changes to the aluminosilicate framework and that selenium can also replace sulfur in "boron" ultramarine with the formation of pink to brown colors.[6-8] The nature of the selenium-containing

(1) Clark, R. J. H.; Cobbold, D. G. *Inorg. Chem.* **1978**, *17*, 3169. Seel, F.; Güttler, H. J. *Angew. Chem., Int. Ed. Engl.* **1973**, *12*, 420.
(2) Holzer, W.; Murphy, W. F.; Bernstein, H. J. *J. Mol. Spectrosc.* **1969**, *32*, 13.
(3) Clark, R. J. H.; Franks, M. L. *Chem. Phys. Lett.* **1975**, *34*, 69.
(4) Chivers, T. In "New Uses of Sulfur"; West, J. R., Ed.; American Chemical Society: Washington DC, 1975; Adv. Chem. Ser. No. 140, pp 499-537.
(5) Berg, R. W.; Bjerrum, N. J.; Papatheodorou, G. N.; Von Winbush, S. *Inorg. Nucl. Chem. Lett.* **1980**, *16*, 201.

0020-1669/83/1322-2766$01.50/0

chromophores has never been established.

The objects of the present work were, by means of electronic and resonance Raman spectroscopy, (a) to investigate the nature of, and relationship between, the chromophores in the various sulfur-containing ultramarines, (b) to establish the nature of the selenium-containing chromophore in ultramarine selenium, (c) to calculate various spectroscopic constants for the radical anions identified, (d) to calculate, by Franck–Condon simulation of the excitation profiles of resonance-enhanced bands, the equilibrium geometries of the anions in their respective resonant-excited states, and (e) to determine the polarization of the resonant electronic transition of S_2^- in the blue solution of Na_2S_4 in DMF. Some features of this work have been reported in preliminary form.[9]

Experimental Section

Materials. The blue solution of Na_2S_4 in dimethylformamide was prepared as described previously.[1] Samples of the various ultramarines, including ultramarine selenium, were provided by Reckitt's Colours Ltd. The ultramarine blue was synthesized from kaolinite and clay, soda ash, sulfur, pitch/oil, and silica by the standard procedure.[6] Treatment of ultramarine blue (Reckitt's grade 06, the finest of the settled grades) with solid $[NH_4]Cl$ (6% by mass) at 225 °C in the presence of air results in the formation of ultramarine violet, which on further treatment with anhydrous HCl at 140 °C for 6 h yields ultramarine pink. The so-called experimental grade I of ultramarine violet was made by first treating ultramarine blue with HCl (100 cm^3 min^{-1}) and air (100 cm^3 min^{-1}) at 225 °C for 5 h and then treating the product with HCl alone (100 cm^3 min^{-1}) at 140 °C for 5 h. Experimental violet grades II and III were made by the same procedure but with different treatment periods at the two stages of the preparation: grade II—stage one, $^1/_4$ h; stage two, 2 h; grade III—stage one, 5 h; no second stage. The most pink form of ultramarine pink is formed by treating ultramarine blue just with chlorine gas at 225 °C to give the violet, followed by treating the latter with anhydrous HCl at 140 °C.

Physical Measurements. Electronic spectra were recorded by using a Cary 14 spectrometer. Raman spectra were recorded by using Spex 1401 (1200 lines mm^{-1}) and 14018 (1800 lines mm^{-1}) spectrometers in conjunction with Coherent Radiation Models CR 3000 K and 500 K (krypton ion) and 12 and 3 (argon ion) lasers. Detection of the scattered radiation was by photon counting, using RCA C31034 photomultipliers. Wavenumber measurements were calibrated by reference to the emission spectrum of neon, and intensities were determined from band areas by using the a_1 band of $K[NO_3]$ or $K_2[SO_4]$ as internal standard, after correction for the spectral response of the appropriate spectrometer.

Raman spectra at 295 K were obtained by the spinning sample technique, from stationary samples at ca. 80 K by use of a liquid nitrogen Dewar assembly and at ca. 10 K by use of an Air Products Displex cryostat.

Results and Discussion

Sulfur-Containing Ultramarines. Ultramarine Blue. Previous work has establiished that both S_3^- and S_2^- are present in ultramarine blue,[1] although the former is in by far the greater amount and thus is primarily responsible for the blue color of the pigment. The present work leads to the same conclusion. The wavenumbers of the members of the $\nu_1\nu_1$ progression of S_3^- for ultramarine blue are independent of sample temperature over the range 300–14 K, as expected. This situation contrasts with that for the ν_1 band of S_3^- and S_2^- in sulfur-doped KI crystals; in this case, the ν_1 bands lower by 10 and 15 cm^{-1}, respectively, over the range 300–20 K (the overtones proportionately more), suggesting that a phase change occurs on lowering the temperature.[10]

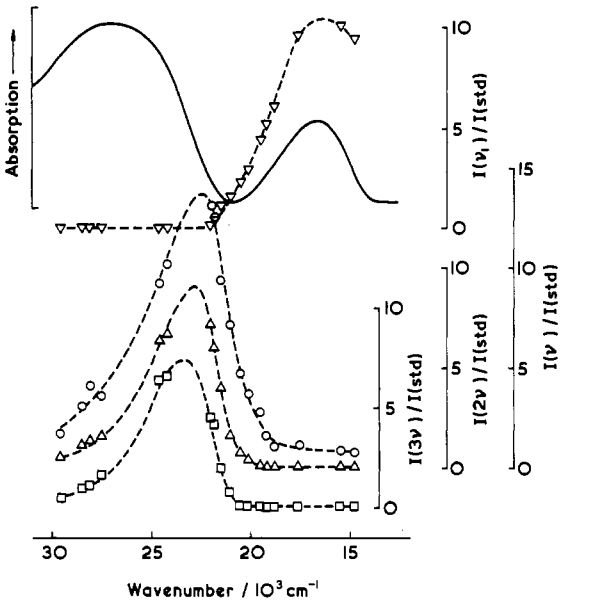

Figure 1. Electronic spectrum (transmission, KBr disk, 14 K) of ultramarine green and the excitation profiles (295 K) of the ν (○), 2ν (△), and 3ν (□) bands of occluded S_2^- and of the ν_1 (▽) band of occluded S_3^-.

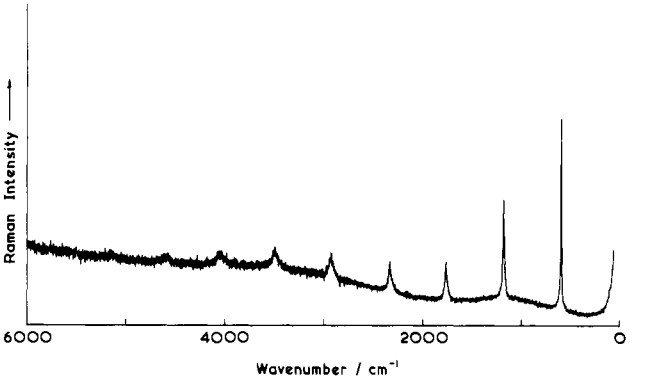

Figure 2. Resonance Raman spectrum of the S_2^- ion in ultramarine green at 295 K with 406.7-nm excitation (slit width ca. 3 cm^{-1}).

Ultramarine Green. The electronic spectrum of ultramarine green at ca. 15 K (Figure 1) indicates that this pigment contains the S_3^- and S_2^- ions in comparable proportions, and no others. The S_3^- ion is, as for ultramarine blue, characterized by the $^2B_1 \leftarrow {}^2A_1$ transition at ca. 600 nm; an Xα–SCF calculation[11] is consistent with this interpretation of the spectrum. The band at ca. 370 nm is assigned to the $^2\Pi_{3/2u}$, $^2\Pi_{1/2u} \leftarrow {}^2\Pi_{3/2g}$ transitions of the S_2^- ion. The $\tilde{\nu}_{00}$ value for this transition has been determined to be 20035 cm^{-1} (499 nm) by fluorescence measurements on sulfur-doped KI crystals.[12-14]

Previous Raman studies on ultramarine green had been restricted on the short-wavelength side to 454.5 nm, a wavelength that barely falls within the contour of the above band of the S_2^- ion. By use of violet (413.1 and 406.7 nm) and ultraviolet (356.7, 350.7, and 337.5 nm) lines of a krypton ion laser, much more intense and detailed resonance Raman spectra of the ion may be obtained. The most intense spectrum (Figure 2) is obtained with 406.7-nm excitation and consists

(6) Jaeger, F. M. *Trans. Faraday Soc.* **1929**, *25*, 320 and references therein.
(7) Hoffmann, J. *Z. Anorg. Allg. Chem.* **1929**, *183*, 37.
(8) Podschus, E.; Hofmann, U.; Leschewski, K. *Z. Anorg. Chem.* **1936**, *228*, 305.
(9) Clark, R. J. H.; Fairclough, D. P.; Kurmoo, M. In "Time-Resolved Vibrational Spectroscopy"; Atkinson, G. H., Ed.; in press.
(10) Holzer, W.; Racine, S.; Cipriani, J. In "Advances in Raman Spectroscopy"; Mathieu, J. P., Ed.; Heyden: London, 1973; Vol. 1, p 393.
(11) Cotton, F. A.; Harmon, J. B.; Hedges, R. M. *J. Am. Chem Soc.* **1976**, *98*, 1417.
(12) Rolfe, J. *J. Chem. Phys.* **1968**, *49*, 4193.
(13) Ikezawa, M.; Rolfe, J. *J. Chem. Phys.* **1973**, *58*, 2024.
(14) Sawicki, C. A.; Fitchen, D. B. *J. Chem. Phys.* **1976**, *65*, 4497.

Table I. Wavenumbers (cm^{-1}), Relative Intensities, and fwhm of the $n\nu$ Progression of S_2^- in Ultramarine Green and of Se_2^- in Ultramarine Selenium

	S_2^- [a]			Se_2^- [b]		
assignt	$\tilde{\nu}$	fwhm	$I(n\nu)/I(\nu)$	$\tilde{\nu}$	fwhm	$I(n\nu)/I(\nu)$
ν	591.2	10	1.00	327.9	9.4	1.00
2ν	1179	20	0.66	655.3	18.9	0.89
3ν	1762	30	0.41	981.4	27	0.84
4ν	2340	40	0.29	1305.9	34	0.78
5ν	2912	48	0.25	1628	43	0.79
6ν	3475	55	0.16	1950	55	0.81
7ν	4035	65	0.10	2266	65	0.63
8ν	4590	>65	<0.10	2585	87	0.58
9ν	5150	>65	<0.10	2900	98	0.55
10ν				3210		
11ν				3520		
12ν				3840		
13ν				4155		

[a] $\lambda_0 = 413.1$ nm; $T = 295$ K. [b] $\lambda_0 = 514.5$ nm; $T =$ ca. 80 K.

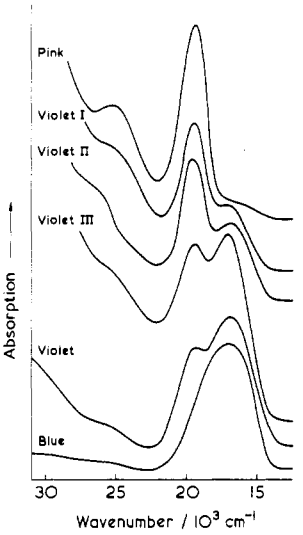

Figure 3. Electronic spectra (transmission, KBr disk, 14 K) of ultramarine blue, violet, experimental violet I, II, and III, and pink.

of a single overtone progression reaching 9ν. These observations are similar to those obtained for S_2^- doped into alkali halide lattices. From the wavenumbers of the members of the progression (Table I), the following spectroscopic data can be calculated by standard procedures: $\omega_e = 597.0 \pm 0.5$ cm^{-1}; $\omega_e x_e = 2.50 \pm 0.15$ cm^{-1}.

The excitation profile of the ν_1 band of S_3^- and of the ν, 2ν, and 3ν bands of S_2^- are shown in Figure 1. Clearly, that of ν_1 of S_3^- follows the contour of the 600-nm electronic band, and those for ν, 2ν, and 3ν of S_2^- follow the contour of the ca. 370-nm band (though significantly red-shifted from it; vide infra).

Ultramarine Violet and Pink. The electronic spectra of the ultramarine blue, the four shades of ultramarine violet (violet and experimental violet I, II, and III) and of ultramarine pink are shown in Figure 3. The principal change in the electronic spectrum on changing from ultramarine blue through the various shades of violet to pink is the increasing prominence of an electronic band at ca. 520 nm at the expense of that at ca. 600 nm (characteristic of the S_3^- ion). The shoulder at 380–400 nm stays roughly of constant intensity in the spectrum of all blue, violet, and pink ultramarines, suggesting that the concentration of the S_2^- ion stays about constant in all these (as opposed to the green) forms of ultramarine. Resonance Raman studies using 406.7-nm excitation demonstrated that the S_2^- ion is the sole chromophore responsible for the 380–400-nm electronic band in all these ultramarines.

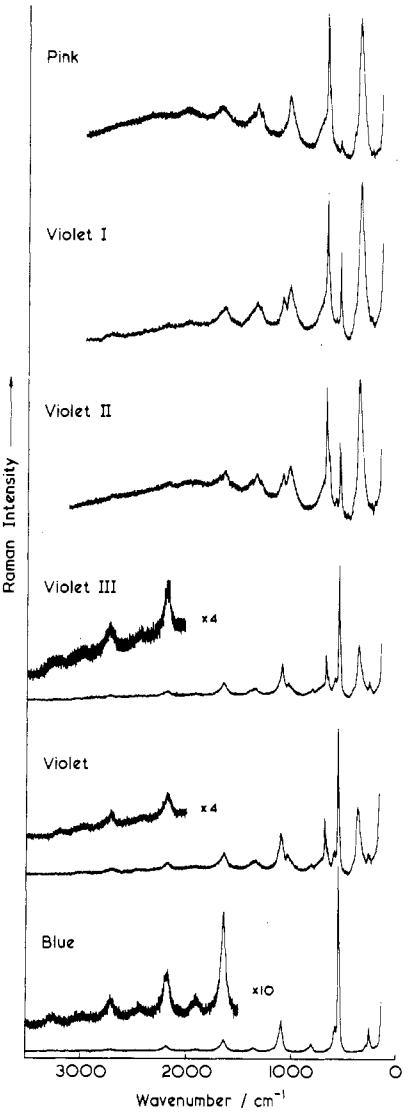

Figure 4. Resonance Raman spectra (295 K) of ultramarine blue, violet, experimental violet I, II, and III, and pink.

Table II. Wavenumbers[a] (cm^{-1}) and Assignments for Bands Observed in the Resonance Raman Spectrum of Ultramarine Pink

$\tilde{\nu}$	assignt	$\tilde{\nu}$	assignt
150 w		1028	674 + 355
355 vs, br		1082	(2 × 546)
410 w, sh		1306	
548 w	$\nu_1(S_3^-)$	1342	(2 × 674)
590[b]	$\nu(S_2^-)$	1382	674 + (2 × 355)
653 m, sh		1680	(2 × 674) + 355 (?)
674 s		1980	
700 vbr	(2 × 355)		

[a] Obtained with 514.5-nm excitation at 295 K. [b] Observed with 457.9-nm excitation.

Simultaneous with the color change from blue through the violets to pink, the resonance Raman spectrum of the pigment is characterized by a buildup of new Raman bands at 355 (vs, br), 410 (w, sh), 653 (m, sh), and 674 (s) cm^{-1} and a decrease in the intensity of the band at 548 cm^{-1} attributed to ν_1 of the S_3^- ion. This result is consistent with the electronic spectral results (vide supra). These resonance Raman spectra are illustrated, for 514.5-nm excitation, in Figure 4. The Raman spectra of ultramarine pink at 295 K for a variety of different excitation lines are shown in Figure 5, the wavenumbers of the observed bands being listed in Table II.

The excitation profiles (Figure 6) of $\nu(S_2^-)$ and $\nu_1(S_3^-)$ bands of ultramarine pink maximize, with their respective electronic

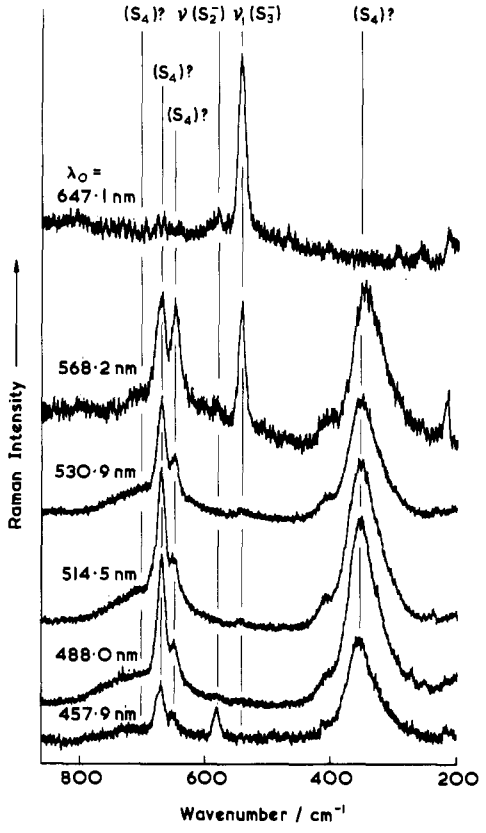

Figure 5. Resonance Raman spectra (295 K) of ultramarine pink for various exciting lines.

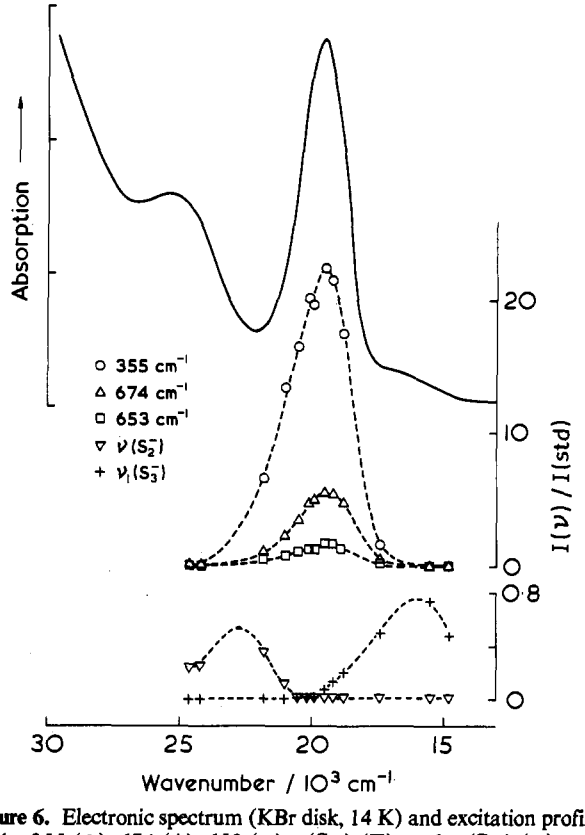

Figure 6. Electronic spectrum (KBr disk, 14 K) and excitation profiles of the 355 (O), 674 (Δ), 653 (□), $\nu(S_2^-)$ (▽), and $\nu_1(S_3^-)$ (+) resonance-enhanced bands of ultramarine pink.

band maxima, in a similar way to that discussed previously for the analogous bands of the same chromophores in ultramarine green. However, those of the 355-, 653-, and 674-cm^{-1} bands maximize with the 520-nm absorption band and clearly

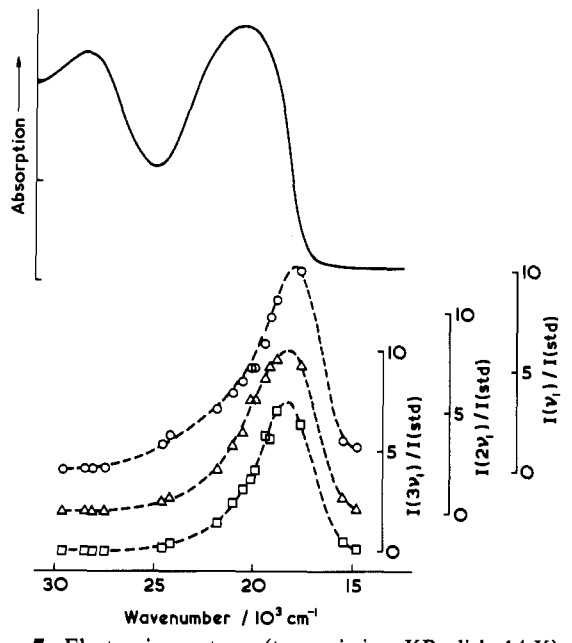

Figure 7. Electronic spectrum (transmission, KBr disk, 14 K) and excitation profiles of ν (O), 2ν (Δ), and 3ν (□) bands of the occluded Se_2^- ion in ultramarine selenium.

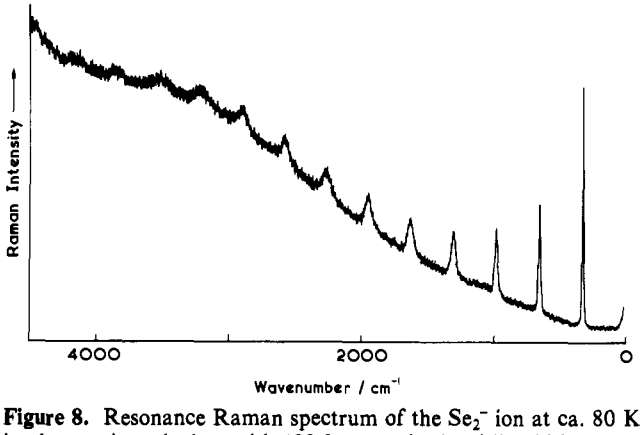

Figure 8. Resonance Raman spectrum of the Se_2^- ion at ca. 80 K in ultramarine selenium with 488.0-nm excitation (slit width ca. 2.5 cm^{-1}).

belong to a further chromophore that must be primarily responsible for the color of this form of ultramarine. Unfortunately, the nature of this species is uncertain, though S_4, S_4^-, ClS_2, and ClS_3 seem possibilities. All the Raman and electronic spectra point to the feasibility of continuously varying the relative proportions of the different chromophores in ultramarine.

Ultramarine Selenium. Ultramarine selenium is brick red and displays two electronic maxima in its electronic spectrum (Figure 7) at 490 and 350 nm. Irradiation of this compound at ca. 80 K within the 490-nm band contour readily yields a resonance Raman spectrum (Figure 8) in which the dominant feature is a long overtone progression in a single mode (ν = 327.9 cm^{-1}), reaching to 13ν with 488.0-nm excitation. This mode can convincingly be identified with the Se–Se stretching mode of the Se_2^- ion by analogy with its value when Se is doped into alkali halide lattices (325 cm^{-1} in KI from Raman measurements and ca. 327 cm^{-1} in KI from fluorescence measurements). The assignment is also supported by the absence of a band attributable to a bending mode (as expected for a possible Se_3^- ion) and of any infrared band. However, the observed resonance Raman progression of Se_2^- in the ultramarine lattice is apparently much longer and more spectacular (Figure 8) than that obtained where an alkali halide acts as the host lattice (in which case the progression

in ν reaches to 3ν only). Standard analysis of the overtone wavenumbers leads to the values $\omega_e = 329.6 \pm 0.3$ cm^{-1} and $\omega_e x_e = 0.70 \pm 0.03$ cm^{-1}, which are in near agreement with the values 329.3 and 0.75 cm^{-1}, respectively, deduced for this ion from fluorescence measurements. It is worth noting that no differences in these constants were noted between measurements made at 295 and 15 K.

The excitation profiles of the ν, 2ν, and 3ν bands of Se_2^- all maximize within the contour of the 490-nm electronic band but, as for the analogous bands of the S_2^- ion (vide supra), are significantly red-shifted from 490 nm. These Raman bands are clearly off resonance at 350 nm, indicating that the ca. 350-nm band of the Se_2^- ion has the opposite polarization to that of the 490-nm band. The latter is assigned to the $^2\Pi_{1/2,3/2u} \leftarrow {}^2\Pi_{3/2g}$ transitions, the $\tilde{\nu}_{00}$ value for which is 16 030 cm^{-1} as deduced from the fluorescence spectrum of the Se_2^- ion in a KI matrix.

There does seem to be a small amount of a further species in ultramarine selenium since, on excitation with either the 350.7-or 356.4-nm lines, two further Raman bands appear, viz. at 375 and 750 cm^{-1} (the latter possibly being the first overtone of the former). This species cannot be the Se_3^- ion, since this would be expected to have its lowest allowed transition at lower energy than that of the Se_2^- ion (cf. S_3^- vs. S_2^-), and since (again by analogy with the corresponding sulfur ions) its symmetric stretch would be expected near 300 cm^{-1}. Indeed, the Se_3^- ion is thought to have been detected in alkali halide lattices,[2] in which matrix its ν_1 value appears to be 280 cm^{-1}. The nature of the minor species responsible for these two weak Raman bands is not known.

Depolarization Measurements on S_2^- in Solution. The depolarization ratio, $\rho(\pi/2)$, of the band assigned to $\nu(S_2^-)$ in the resonance Raman spectrum of Na_2S_4 in DMF solution was found to be 0.14 ± 0.03 for 406.7-, 413.1-, and 457.9-nm excitation. These three excitation wavelengths are close to that of the absorption maximum corresponding to the $^2\Pi_u \leftarrow {}^2\Pi_g$ transition for S_2^-, and within experimental error $\rho(\pi/2)$ is identical with the value of $^1/_8$ predicted for excitation in resonance with an (x,y)-polarized transition. In the absence of spin–orbit interaction, the $^2\Pi_u \leftarrow {}^2\Pi_g$ transition would be expected to be z polarized ($\Pi_u \times \Pi_g = \Sigma_u^+ + \Sigma_u^- + \Delta_u$), from which we would expect that $\rho(\pi/2) = {}^1/_3$. However, the spin–orbit coupling constant, λ, is 420 cm^{-1} for S_2^-,[15] resulting in a splitting of the $^2\Pi$ states into $^2\Pi_{1/2}$ and $^2\Pi_{3/2}$ components (as is the case for the NO molecule). The ground state of S_2^- is $^2\Pi_{3/2g}$[16] and the $^2\Pi_{3/2u}$, $^2\Pi_{1/2u} \leftarrow {}^2\Pi_{3/2g}$ transitions contain both z- and (x,y)-polarized components ($^2\Pi_{1/2u} \times {}^2\Pi_{3/2g} = \Pi_u + \Delta_u$ and $^2\Pi_{3/2u} \times {}^2\Pi_{3/2g} = \Sigma_u^+ + \Sigma_u^- + \Pi_u$). The measured depolarization ratio indicates that the (x,y)-polarized component is much more intense than the z-polarized one.

In principle, it should be possible to observe an electronic Raman band at around 400 cm^{-1} corresponding to the $^2\Pi_{1/2g} \leftarrow {}^2\Pi_{3/2g}$ transition (analogous to the 122-cm^{-1} band observed in the gas-phase Raman spectrum of NO, assigned to $^2\Pi_{3/2g} \leftarrow {}^2\Pi_{1/2g}$[17]). The absence of such a band may not be surprising because electronic bands observed in the Raman spectra of solution species at room temperature tend to be very broad.[18]

Stress-induced linear dichroism (SLD) studies of S_2^- and Se_2^- in a KI host lattice have been performed,[19] and from the signs of the SLDs it is deduced that the lowest energy electronic transitions in S_2^- and Se_2^- are z polarized. This is due to crystal-field splitting of the $^2\Pi$ states into B_2 and B_3 components in the KI lattice, where the radicals occupy sites of D_{2h} symmetry. The ground state becomes B_{3g}, and the only allowed transition is to the B_{2u} component of the excited state and thus is z polarized ($B_{2u} \times B_{3g} = B_{1u}$). In the ultramarines the radicals occupy cubic sites and no crystal-field splitting of the $^2\Pi$ states is expected to occur, although there will be spin–orbit interactions, as for the species in solution.[15]

Table III. Parameters Used in the Calculations of the Resonance Raman Excitation Profiles and Overtone Intensity Distributions

parameter	S_2^-	Se_2^-	source
$\tilde{\nu}^g$/cm^{-1}	591	328	Raman spectrum
$\tilde{\nu}^e$/cm^{-1}	360	216	absorption spectrum in KI[15]
$\tilde{\nu}_{eg}$/cm^{-1}	20100 ± 50	16500 ± 100	best fit[a]
Δr/Å	0.30 ± 0.01	0.32 ± 0.02	best fit
Γ/cm^{-1}	300 ± 50	150 ± 50	best fit
γ/cm^{-1}	400 ± 50	400 ± 100	best fit

[a] The wavenumber of the 0–0 transition has been measured from luminescence spectra for S_2^- in a number of different alkali halide lattices and for Se_2^- in KI.[15] For S_2^- a range of values between 19 000 and 21 000 cm^{-1} are obtained depending on the host lattice, and for Se_2^- in KI the 0–0 transition is at 16 030 cm^{-1}.

Calculations of Band Excitation Profiles. Using an established theoretical model, we have attempted to determine the changes of bond length that accompany excitation to the $^2\Pi_u$ states of S_2^- and Se_2^-, by computer simulation of their excitation profiles. Such a procedure has been used successfully for the species $[MnO_4]^-$[20] and $[MoS_4]^{2-}$[21] where vibronic structure is observed in both the electronic absorption spectra and resonance Raman excitation profiles. Although the $^2\Pi_u \leftarrow {}^2\Pi_g$ absorption bands of S_2^- and Se_2^- in the ultramarine host lattice exhibit no vibronic structure, even at 14 K, we have been able to perform calculations by using certain parameters obtained from absorption and luminescence studies of S_2^- and Se_2^- in the KI host lattice.[15]

The Raman intensity for 90° scattering geometry, resulting from a transition between the two states $|i\rangle$ and $|f\rangle$ of the scattering system, is given by

$$I\left(\frac{\pi}{2}\right) = 10^8 \frac{\pi^2}{\epsilon_0^2}(\tilde{\nu}_0 \pm \tilde{\nu}_{fi})^4 \mathcal{J}_0 \sum_{\rho\sigma} [\alpha_{\rho\sigma}]_{fi}[\alpha_{\rho\sigma}]_{fi}^* \qquad (1)$$

where $\mathcal{J}_0$/W m^{-2} is the irradiance of the incident radiation of wavenumber $\tilde{\nu}_0$/cm^{-1}, $\tilde{\nu}_{fi}$ is the wavenumber associated with the Raman transition $|f\rangle \leftarrow |i\rangle$, ϵ_0/(F m^{-1}) is the permittivity of free space, and $[\alpha_{\rho\sigma}]_{fi}$ is the $\rho\sigma$th element of the transition polarizability tensor, which is given by

$$[\alpha_{\rho\sigma}]_{fi} = \frac{1}{hc}\sum_r \left\{ \frac{[\mu_\rho]_{fr}[\mu_\sigma]_{ri}}{\tilde{\nu}_{ri} - \tilde{\nu}_0 + i\Gamma_r} + \frac{[\mu_\sigma]_{fr}[\mu_\rho]_{ri}}{\tilde{\nu}_{fr} + \tilde{\nu}_0 + i\Gamma_r} \right\} \qquad (2)$$

$[\mu_\rho]_{fr}$ is the ρth component of the transition dipole moment associated with the transition $|f\rangle \leftarrow |r\rangle$; Γ_r is a damping factor (which is inversely proportional to the lifetime of the state $|r\rangle$) and the summation is over all states $|r\rangle$ of the system, excluding $|i\rangle$ and $|f\rangle$. Under the conditions for which the Born–Oppenheimer approximation is valid, the states $|i\rangle$, $|f\rangle$, and $|r\rangle$ may be expressed as products of vibrational and electronic states. Since the resonant electronic transitions of S_2^- and Se_2^- are strongly electric dipole allowed, we may also invoke the Condon approximation; i.e., the dependence of the transition dipole moment on the nuclear coordinates is neglected (A-term

(15) Vella, G. J.; Rolfe, J. *J. Chem. Phys.* **1974**, *61*, 41.
(16) Vannotti, L. E.; Morton, J. R. *Phys. Rev.* **1967**, *161*, 282.
(17) Rasetti, F. *Z. Phys.* **1930**, *66*, 646.
(18) Clark, R. J. H.; Dines, T. J. In "Advances in Infrared and Raman Spectroscopy"; Clark, R. J. H., Hester, R. E., Eds.; Heyden: London, 1982; Vol. 9, Chapter 5.
(19) Boccara, A. C.; Duran, J.; Briat, B.; Stephens, P. J. *Chem. Phys. Lett.* **1973**, *19*, 187.
(20) Clark, R. J. H.; Stewart, B. *J. Am. Chem. Soc.* **1981**, *103*, 6593.
(21) Clark, R. J. H.; Dines, T. J.; Wolf, M. L. *J. Chem. Soc., Faraday Trans. 2* **1982**, *78*, 679.

Table IV. Overtone Intensity Distribution for the $n\nu$ Progression of S_2^- and Se_2^-

	S_2^-				Se_2^-			
	obsd[a]	calcd	obsd[a]	calcd	obsd[a]	calcd	obsd[a]	calcd
λ_0/nm	457.9	457.9	413.1	413.1	568.2	568.2	514.5	514.5
ν	1.00	1.000	1.00	1.000	1.00	1.00	1.00	1.00
2ν	0.52	0.464	0.66	0.384	0.74	0.54	0.95	0.98
3ν	0.29	0.300	0.41	0.244	0.58	0.35	0.87	0.55
4ν	0.17	0.222	0.29	0.166	0.52	0.25	0.71	0.46
5ν	0.10	0.165	0.25	0.120	0.40	0.21	0.68	0.37
6ν		0.124	0.16	0.097			0.57	0.28
7ν		0.099	0.10	0.076				
8ν			<0.10	0.063				
9ν			<0.10	0.054				

[a] 295 K.

resonance Raman scattering). This enables the transition polarizability for a totally symmetric vibrational Raman transition to be expressed as

$$[\alpha_{\rho\rho}]_{gn,gm} = \frac{1}{hc}|[\mu_\rho]_{ge}{}^0|^2\sum_v \langle n_g|v_e\rangle\langle v_e|m_g\rangle/(\tilde{\nu}_{ev,gm} - \tilde{\nu}_0 + i\Gamma_{ev}) \quad (3)$$

where $|g\rangle$ and $|e\rangle$ are respectively the ground electronic state and the resonant excited state, m_g and n_g are the initial and final vibrational quantum numbers, respectively, and the summation is over all vibrational quanta v_e of the excited state. The nonresonant term in eq 2 has been neglected because its contribution is very small under resonance conditions.

Calculations of excitation profiles (EPs) for the fundamental Raman band and its overtones may be performed by using eq 1 and 3 and substituting values for $\tilde{\nu}_{ev,gm}$, $\tilde{\nu}_{gn,gm}$, $\tilde{\nu}_0$, Γ_{ev}, and the Frank–Condon factors $\langle n_g|v_e\rangle\langle v_e|m_g\rangle$ (all other quantitites are wavenumber independent). The vibrational overlap integrals, which are calculated by using Manneback's recursion formulas,[22] are dependent on the ground-state and excited-state vibrational wavenumbers and the displacement of the excited-state potential minimum with respect to that of the ground state along the vibrational coordinate. This displacement is related to the change in bond length accompanying electronic excitation. The resonant electronic transition in S_2^- and Se_2^- is expected to produce an increase in bond length since the promotion of an electron from the π_u bonding orbital to the π_g antibonding orbital reduces the bond order from 1.5 to 1.

By the calculation of best fit EPs to the experimentally determined points for S_2^- and Se_2^-, it was found that in both cases the bond length extension on excitation, Δr, was approximately 0.3 Å. However, the calculations failed to reproduce satisfactorily the observed intensity distribution of the overtone progressions and necessitated the use of unacceptably large values of Γ (in the range 500–700 cm^{-1}). This is because the broadening of the unresolved EPs of $\nu(S_2^-)$ and $\nu(Se_2^-)$ in the ultramarine lattice is due, not only to lifetime (homogeneous) broadening, but also to inhomogeneous broadening deriving from variations in the interaction of the radical anion with the host lattice. It is necessary to consider, therefore, the variation of the electronic transition wavenumber, $\tilde{\nu}_{eg}$, induced by the molecular environment, which is assumed to be described by a Lorentzian distribution

$$\mathcal{L}(\tilde{\nu}_{eg}) = \frac{\gamma}{(\tilde{\nu}_{eg} - \langle\tilde{\nu}_{eg}\rangle)^2 + \gamma^2} \quad (4)$$

where $\langle\tilde{\nu}_{eg}\rangle$ is the average value of the transition wavenumber and γ is the half-width associated with the inhomogeneous broadening mechanism. The transition polarizability is then given by

$$[\alpha_{\rho\rho}]_{gn,gm} = \frac{1}{hc}|[\mu_\rho]_{ge}{}^0|^2\int_{-\infty}^{\infty}\left[\sum_v \frac{\langle n_g|v_e\rangle\langle v_e|m_g\rangle}{\tilde{\nu}_{ev,gm} - \tilde{\nu}_0 + i\Gamma_{ev}}\right]\mathcal{L}(\tilde{\nu}_{eg})\, d\tilde{\nu}_{eg} \quad (5)$$

Siebrand and co-workers[23,24] have evaluated such integrals, and excitation profiles may be determined from the following equation:

$$I_{gn,gm}\left(\frac{\pi}{2}\right) = K(\tilde{\nu}_0 - \tilde{\nu}_{gn,gm})^4\sum_m \exp\left(-\frac{hc\tilde{\nu}^g}{kT}\right) \times \left[1 - \exp\left(-\frac{hc\tilde{\nu}^g}{kT}\right)\right]\sum_v\sum_{v'}\langle n_g|v_e\rangle\langle v_e|m_g\rangle\langle n_g|v_e'\rangle\langle v_e'|m_g\rangle\Gamma \times \{[(\epsilon_v - \epsilon_v')^2 + 4\Gamma(\Gamma + \gamma)] \times [\epsilon_v\epsilon_v' + (\Gamma + \gamma)^2] - 2(\epsilon_v - \epsilon_v')\gamma(\Gamma + \gamma)\}/\{[\epsilon_v^2 + (\Gamma + \gamma)^2][\epsilon_v'^2 + (\Gamma + \gamma)^2][(\epsilon_v - \epsilon_v')^2 + 4\Gamma^2]\} \quad (6)$$

where $\epsilon_v = \tilde{\nu}_{ev,g0} - \tilde{\nu}_0$, $\tilde{\nu}^g$ is the vibrational wavenumber in the ground electronic state, and a common homogeneous line width Γ has been taken for all of the excited-state vibrational levels.

Calculations of the resonance Raman excitation profiles and overtone intensity distributions from eq 6 provide a substan-

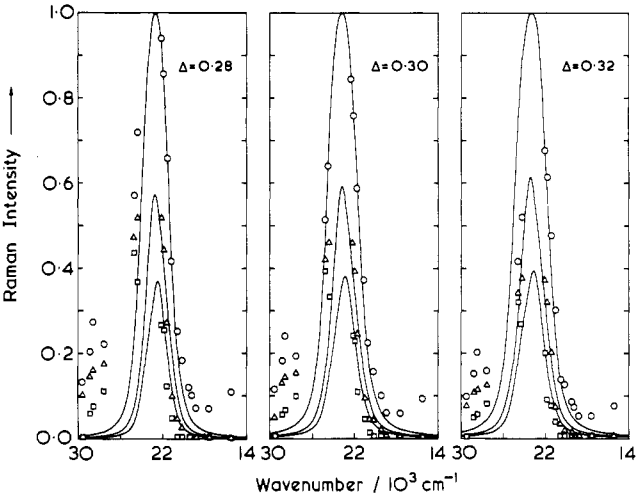

Figure 9. Experimental excitation profiles of the ν (○), 2ν (△), and 3ν (□) bands of the S_2^- ion in ultramarine green and calculated profiles (solid lines) for Δr = (a) 0.28, (b) 0.30, and (c) 0.32 Å (Γ = 300 and γ = 400 cm^{-1} in each case). The observed intensity of the ν band using 454.5-nm excitation has been set equal to the calculated intensity at this wavelength for each value of Δr, and the band intensities at other wavelengths were scaled accordingly.

(22) Manneback, C. *Physica (Amsterdam)* **1951**, *17*, 1001.

(23) Penner, A. P.; Siebrand, W. *Chem. Phys. Lett.* **1976**, *39*, 11.
(24) Siebrand, W.; Zgierski, M. Z. *J. Phys. Chem.* **1982**, *86*, 4718.

tially better fit to the experimental data than did those in which inhomogeneous broadening is neglected. The values of the parameters involved in the calculations are listed in Table III and the best fit calculated EPs for S_2^- are shown in Figure 9. Table IV provides a comparison of calculated and experimental overtone intensity distributions of both S_2^- and Se_2^- for selected excitation wavelengths. The following observations may be made:

(1) The quality of the fit of the calculated to the experimental data becomes inferior on the high wavenumber side of the EP maximum. This may be due to contributions to the transition polarizability from higher energy electronic transitions.

(2) The quality of the fit is better for S_2^- than for Se_2^-, which might reflect the greater importance of higher energy contributions for the latter.

(3) The bond length changes attendant upon electronic excitation are similar to that found for iodine[25] (0.35 Å for $^3\Pi_{0u}^+ \leftarrow {}^1\Sigma_g^+$ excitation), but substantially greater than those determined for tetrahedral species (e.g., Δr = 0.09 Å for $[MnO_4]^-$[20] and 0.07 Å for $[MoS_4]^{2-}$[21]). This is due to the much larger reduction in bond order occurring for electronic excitation of diatomic species. Additional evidence for this is furnished by the substantial reduction of the vibrational wavenumber in the excited state, ca. 45% for S_2^- and 40% for Se_2^-. By contrast, the wavenumbers of the totally symmetric fundamentals of tetrahedral molecules decrease by only about 10% on excitation to the lowest energy charge-transfer state.

(25) Herzberg, G. "Spectra of Diatomic Molecules"; Van Nostrand: New York, 1950; p 54.

Conclusion

The results suggest that the ultramarine lattice is an extremely useful matrix with which to trap and to study otherwise unstable inorganic radicals. Its further potential in this respect is the subject of continuing studies.

Acknowledgment. We thank the S.E.R.C. and the University of London for financial support and Reckitt's Colours Ltd. (in particular W. B. Cork) for supplying samples of the various ultramarines and for details on their manufacture.

Registry No. Ultramarine green, 1345-00-2; ultramarine blue, 57455-37-5; ultramarine violet, 12769-96-9; ultramarine pink, 12769-96-9; ultramarine selenium, 86595-02-0.

Notes

Contribution from the Department of Chemistry, University of Otago, Dunedin, New Zealand

Reversed-Phase High-Performance Liquid Chromatography of Cobalt(III) Complexes. Concentration-Dependent Splitting of Single Species

D. A. Buckingham,* C. R. Clark, and R. F. Tasker

Received December 29, 1982

Recently, during studies on ion pair RP-HPLC of Δ-$[Co(en)_2(AA)]^{2+}$ (AA = amino acid) mixtures, we found conditions that allowed single species to completely split into two.[1] This caused us some early misgivings, but the clear advantages this technique has in separating mixtures of closely related cobalt(III) species[2] made us look at this peak-splitting problem in a little more detail. It results from the association of two (or more) complex ions, the ion-pairing reagent and the stationary phase, and is most apparent at low pairing-ion concentrations. It differs from other induced-peak phenomena,[3] which have their origins in sudden solvent–eluent changes; it is potentially more prone to misinterpretation. The following results may be of value to those contemplating the use of RP-HPLC for separating charged metal complexes.

Results and Discussion

Figure 1a shows the rapid and complete separation of five Δ-$[Co(en)_2(AA)]^{2+}$ complexes, in order of elution AA = Gly, Pro, Val, Leu, Phe. When the sample loading is increased at constant ion-pairing conditions (5 mM tosylate, pH 3.50) (Figure 1b,c), the AA = Gly and Pro peaks each split into two with the earlier major components preceding, with progressively shorter retention times (t_R(abnormal)), the minor components, which have normal retention times (t_R(normal)). The degree of splitting, $\Delta t_R = t_R(\text{normal}) - t_R(\text{abnormal})$, is related to the *total amount* of complex loaded rather than to an excess of any one species. Figure 2 demonstrates this with increasing amounts of AA = Pro, causing splitting of the AA = Gly component at constant Gly loading before it itself is split. This effect is clearly distinguished from "normal" overloading, which

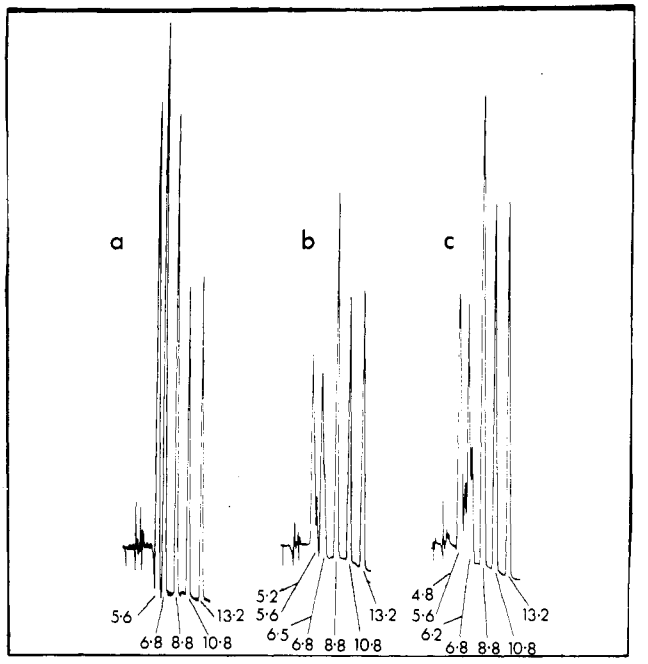

Figure 1. Chromatograms of Δ-$[Co(en)_2(AA)]I_2$ complexes where AA = Gly, Pro, Val, Leu, Phe in order of elution (0–100% $MeOH/H_2O$ eluent over 15 min (linear); 5 mM tosylate, pH 3.5; flow rate 2.5 cm^3 min^{-1}; t_R in min). Increased loadings [(a) 367 nmol (10 μL), (b) 734 nmol (20 μL), (c) 1001 nmol (30 μL)] result in splitting of AA = Gly, t_R(normal) = 5.6, t_R(abnormal) = 5.2 (b), 4.8 (c), and of AA = pro, t_R(normal) = 6.8, t_R(abnormal) = 6.5 (b), 6.2 (c).

(1) Buckingham, D. A.; Clark, C. R.; Tasker, R. F.; Hearn, M. T. W. *J. Liq. Chromatogr.* **1981**, *4*, 689.

(2) The main advantages are speed of separation, resolution, and small sample size (μg–mg).[6] It is to be noted that samples were made up in doubly distilled deionized water and were carefully filtered before injection.

(3) Tseng, P. K.; Rogers, L. B. *J. Chromatogr. Sci.* **1978**, *16*, 436. Stranahan, J. J.; Deming, S. N. *Anal. Chem.* **1982**, *54*, 1540 and references therein.

0020-1669/83/1322-2772$01.50/0